Effects of final state interactions on charge separation in relativistic heavy ion collisions

Guo-Liang Ma[a], Bin Zhang[b]

[a] *Shanghai Institute of Applied Physics, Chinese Academy of Sciences, Shanghai 201800, China*

[b] *Department of Chemistry and Physics, Arkansas State University, P.O. Box 419, State University, AR 72467-0419, USA*

Abstract

Charge separation is an important consequence of the Chiral Magnetic Effect. Within the framework of a multi-phase transport model, the effects of final state interactions on initial charge separation are studied. We demonstrate that charge separation can be significantly reduced by the evolution of the Quark-Gluon Plasma produced in relativistic heavy ion collisions. Hadronization and resonance decay can also affect charge separation. Moreover, our results show that the Chiral Magnetic Effect leads to the modification of the relation between the charge azimuthal correlation and the elliptic flow that is expected from transverse momentum conservation only. The transverse momentum and pseudorapidity dependences of, and the effects of background on the charge azimuthal correlation are also discussed.

Keywords: Charge separation, parton cascade, resonance decay
PACS: 25.75.-q, 24.10.Lx, 25.75.Gz, 25.75.Ld

1. Introduction

Charge separation along the angular momentum direction has been investigated in relativistic heavy ion collisions [1, 2]. The experimental study was motivated by the theoretical investigation of the Chiral Magnetic Effect [3–10]. The Chiral Magnetic Effect is related to the fact that the hot and dense

Email addresses: glma@sinap.ac.cn. (Guo-Liang Ma[a]), bzhang@astate.edu. (Bin Zhang[b])

matter created in heavy ion collisions can form $\mathcal{P}$ and $\mathcal{CP}$ odd metastable domains where the parity and time-reversal symmetries are locally violated. In the early stage of a non-central relativistic heavy ion collision, the magnetic field can reach a magnitude on the order of 10^{15} T. In the presence of a strong magnetic field, these topologically non-trivial domains impose constraints on quark chiralities and induce a separation of negative and positive particles in the direction of magnetic field (i.e. system angular momentum). In spite of large theory uncertainties, the experimental results are consistent with Chiral Magnetic Effect expectations.

In addition to the Chiral Magnetic Effect, other effects can also contribute to charge separation and/or charge correlation. Bzdak et al. found that the contribution due to transverse momentum conservation is comparable in magnitude to the prediction of the Chiral Magnetic Effect as well as the data [11]. Wang also argued that the measured data can be accounted for by cluster particle correlations and new physics may not be required to explain the data [12]. Schlichting and Pratt argued that local charge conservation, when combined with elliptic flow, explains much of experimental measurements [13]. To our knowledge, no previous studies have included the dynamical effects of final state interactions, such as parton cascade and resonance decay, on the experimental charge separation observable. On the other hand, these final state interaction effects have been found important for many experimental observables, such as elliptic flow and particle yields. In the following, we will address the problem of whether an initial charge separation will be able to survive the final state interactions.

The paper is organized as follows. In Section 2, we give a brief description of A Multi-Phase Transport (AMPT) model and its adaptation for the study of charge separation. Results on the charge separation observable are presented in Section 3 followed by a summary in Section 4.

2. A Multi-Phase Transport model

The AMPT model [14–16] is a dynamical transport model that includes four different stages in relativistic heavy ion collisions: the initial condition, partonic interactions, the conversion from partonic matter into hadronic matter, and hadronic rescatterings. The initial condition, which includes the spatial and momentum distributions of minijet partons and soft string excitations, is obtained from the Heavy Ion Jet INteraction Generator (HIJING) model [17, 18]. There are two options for doing the parton evolution

and hadronization in the AMPT model. One option is the default model which includes only interactions of minijet gluons via Zhang's Parton Cascade (ZPC) [19] and uses the Lund string fragmentation model [20] to turn partons into hadrons. The other option is the string melting model. It starts the parton evolution with a quark-anti-quark plasma from the dissociation of strings. It recombines partons via a simple coalescence model to produce hadrons [22]. Dynamics of the subsequent hadronic matter is then described by A Relativistic Transport (ART) model [21]. The default model has good agreement of particle spectra with experimental data but it significantly underestimates the elliptic flow. In contrast, the string melting model can only describe low transverse momentum spectra, but the agreement with the elliptic flow data is much better. In addition, the AMPT model has been used to study other observables, such as strangeness [23, 24], charm [25], J/Ψ production [26–28], two-pion correlation function [29], dijet correlations [30, 31], triangular and higher order flows [32, 33].

The AMPT model with string melting starts with a quark-anti-quark plasma and it will be used for the study of the effects of final state interactions on charge separation. The Chiral Magnetic Effect is not built into the AMPT model. In order to separate a fraction of the charges initially, we switch the p_y values of a fraction of the downward moving u quarks with those of the upward moving $\bar{u}$ quarks, and likewise for $\bar{d}$ and d quarks. The coordinate system is set up so that the x-axis is in the reaction plane and the y-axis is perpendicular to the reaction plane with the z-axis being the incoming direction of one nucleus. The above procedure ensures total momentum conservation while giving momentum kicks to produce an upward initial current. The current implementation of the ART model does not conserve the electric charge. In the following, we turn off the hadron evolution. The strong parton cascade provides the most contribution to the evolution and the exclusion of hadron evolution in the string melting model is not expected to make significant changes to the final results. Resonance decays are implemented to ensure charge conservation and are included for the study of charge correlations.

3. Charge separation in heavy ion collisions

To measure charge separation possibly coming from local strong parity violation in relativistic heavy-ion collisions, the STAR experiment studied a charge azimuthal correlation observable $\langle\cos(\phi_\alpha + \phi_\beta - 2\Psi_{RP})\rangle$ as proposed

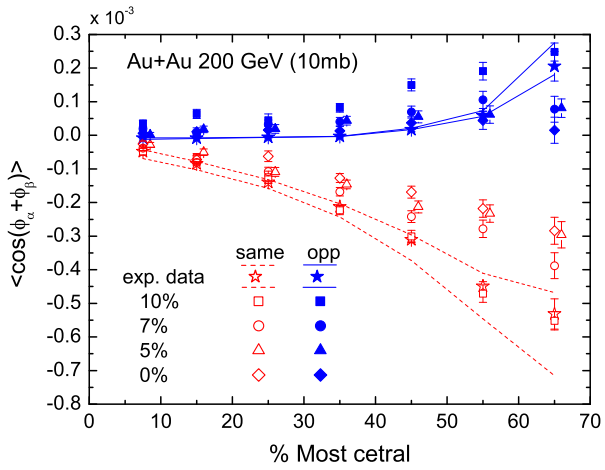

Figure 1: Centrality dependence of $\langle\cos(\phi_\alpha + \phi_\beta)\rangle$ in Au+Au collisions at $\sqrt{s_{\rm NN}}$=200 GeV (with a 10 mb parton cross section). The different symbols represent different percentages of initial charge separation in AMPT calculations. The stars represent experimental data, where the two surrounding curves give the systematic uncertainty for data. Some points are slightly shifted for clarity.

by Voloshin [34]. Here, α and β represent the signs of electric charges and can be positive or negative, while Ψ_{RP} is the azimuthal angle of the reaction plane. By measuring the correlations for same-charge and opposite-charge pairs, the data show some hints of charge separation, which is consistent with the expectation of the Chiral Magnetic Effect [1, 2]. In the following, we will look at how the initial charge separation contributes to the charge azimuthal correlation. The reaction plane azimuthal angle will be set to zero degrees. Au+Au collisions at $\sqrt{s_{\rm NN}}$ = 200 GeV with a 10 mb parton cross will be studied and light quark and charged pion correlations will be analyzed.

Fig. 1 presents the charge azimuthal correlation as a function of centrality from the AMPT simulations. Since the initial charge separation could depend on centrality, different percentages of initial charge separation are used for each centrality bin to look for possible centrality dependence. The STAR correlation data are also shown for comparison. For the same-charge correlation, results from the AMPT model without initial charge separation have smaller magnitudes than data. As the percentage of initial charge separation increases, the magnitude of the correlation increases. The increase is

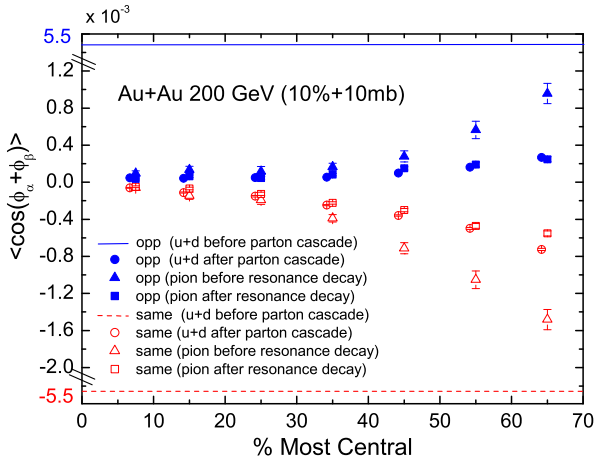

Figure 2: Centrality dependence of $\langle\cos(\phi_\alpha + \phi_\beta)\rangle$ for different stages in AMPT calculations with an initial charge separation percentage of 10% for Au+Au collisions at $\sqrt{s_{\rm NN}}$=200 GeV (with a 10 mb parton cross section). Some points are slightly shifted for clarity.

not linear in the initial charge separation percentage. A percentage of 10% for initial charge separation can describe well the STAR measurements. For the opposite-charge correlation, it seems that initial charge separation is not necessary for all centralities except the most peripheral bin of 60-70%. For the centrality bin of 60-70%, a percentage of 10% is indeed needed to match the experimental observation. In other words, the observed opposite-charge correlation changes much faster than the AMPT results. Even though 10% initial charge separation can describe both the same-charge and opposite-charge correlations for the 60%-70% centrality bin, it is difficult to describe the centrality dependence of both the same-sign and opposite-sign correlations with initial charge separation alone. We also notice that the results with 5% initial charge separation are almost identical to those without initial charge separation. This indicates that it might be challenging to observe an initial charge separation of 5% or less in the presense of strong final state interactions.

To understand how the charge correlation observable evolves in heavy-ion collisions, Fig. 2 shows the centrality dependence of charge correlations for different stages in the AMPT model. With an initial percentage of 10%

charge separation, the initial charge correlations are quite large (solid and dash lines), with a magnitude of about 5.5×10^{-3}. After strong parton cascade, charge correlations are significantly reduced especially for central collisions because of frequent parton interactions under high parton density. The charge correlations are recovered partly from hadronization as coalescence reduces the number of particles while combining quarks into hadrons. Resonance decays act opposite to coalescence and reduce charge correlations in the hadronic phase. The final charged pion correlations have magnitudes comparable with those of final partons. Related to the charge correlation is the percentage of charge separation. Its centrality dependence has the same qualitative evolution where parton cascade and resonance decay decrease while coalescence increases the percentage. From a percentage of charge separation of 10% in the beginning, only 1-2% percentage remains at the end with more peripheral collisions having larger percentages.

As a comparison, the charge correlations at different stages with no initial charge separation are shown in Fig. 3 for different centrality bins. Before the parton cascade, both the same-charge and the opposite-charge correlations are consistent with zero. After the parton stage, both correlations become negative with the same-charge correlation having the larger magnitude. Negative correlations indicate that the correlated charges move together and they are not separated. Coalescence increases the magnitude for the same-charge correlation and resonance decay decreases it as in the case with a non-zero initial charge separation. However, for opposite charges, coalescence reduces the correlation. If the opposite-charge correlation is calculated including charged rho mesons in addition to charged pions, it has a magnitude that is larger than that of quarks after parton cascade. This shows that when there is no initial charge separation, the opposite-charge correlation from coalescence is not equally distributed among different species combinations.

Recently, Bzdak et al. found that transverse momentum conservation can contribute to the charge correlations with magnitudes comparable to experimentally observed correlations [11]. The charge correlations can be calculated from transverse momentum conservation alone. Under the assumption that all particles have the same average transverse momentum, there is a simple relation between the charge correlations and the elliptic flow. Both the same-charge and opposite-charge correlations are equal to $-v_2/N$ for sufficiently large N. Here v_2 is the elliptic flow coefficient and N is the total number of produced particles (similar results were also obtained in [35, 36]). The opposite-charge correlation can be affected by factors other than trans-

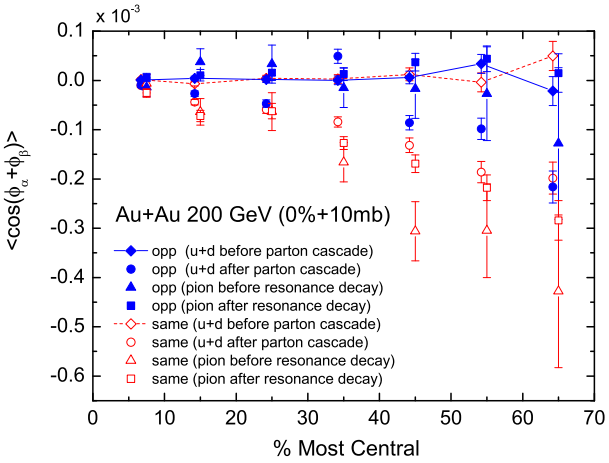

Figure 3: Centrality dependence of $\langle\cos(\phi_\alpha + \phi_\beta)\rangle$ for different stages from AMPT calculations without initial charge separation for Au+Au collisions at $\sqrt{s_{\rm NN}}$=200 GeV (with a 10 mb parton cross section). Some points are slightly shifted for clarity.

verse momentum conservation. In the following, we will look at how this relation holds for the same-charge correlation. Fig. 4 presents the same-charge correlation as a function of $-v_2/N$ for different stages from AMPT calculations without (0%, open symbols) and with (10%, solid symbols) initial charge separation. Here v_2 and N are for particles with pseudorapidity $|\eta|$ <1. The AMPT results without initial charge separation are consistent with the expectation that $\langle\cos(\phi_\alpha + \phi_\beta)\rangle = -v_2/N$, which is shown in the figure by a dashed line. It indicates that the same-charge correlation is driven by transverse momentum conservation in the AMPT model without initial charge separation. On the other hand, the AMPT results with initial charge separation are much lower than the expected relation. It is interesting to see that the linear relation between the same-charge correlation and $-v_2/N$ is approximately preserved with a coefficient much large than 1. Since the AMPT results with 10% initial charge separation can describe the same-charge correlation data well as shown in Fig. 1, transverse momentum conservation can only partly account for the measured charge correlation data.

In more detail, Fig. 5 shows the dependences of charge correlations on the average of the transverse momentum ($p_+ = (p_{t,\alpha} + p_{t,\beta})/2$) of two final charged pions for the 30-50% centrality bin. For the same-charge correla-

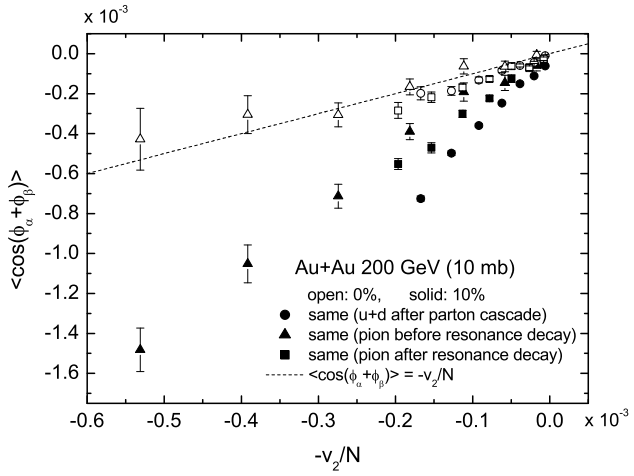

Figure 4: $\langle\cos(\phi_\alpha + \phi_\beta)\rangle$ as a function of $-v_2/N$ for different stages in AMPT calculations without (0%, open symbols) and with (10%, solid symbols) initial charge separation for Au+Au collisions at $\sqrt{s_{\rm NN}}$=200 GeV (with a 10 mb parton cross section). The dashed line represents the relation of $\langle\cos(\phi_\alpha + \phi_\beta)\rangle = -v_2/N$.

tion, the magnitudes of results from the AMPT model without initial charge separation are smaller than those of data while 10% initial charge separation can increase the magnitudes to reproduce data. For opposite-charge pairs, the correlation with no initial charge separation is consistent with data while the correlation with 10% initial charge separation increases weakly with p_+ and is a little higher than data. All of these results are consistent with the integrated correlations which are presented in Fig. 1. From transverse momentum conservation, $\langle\cos(\phi_\alpha + \phi_\beta)\rangle$ is proportional to p_+^n with $n = 2$ to 3 [11]. The curves in Fig. 5 show the power-law fits to the same-charge correlations from the AMPT model. The power n is 2.24 $\pm$ 0.27 when there is no initial charge separation, consistent with the expectation from transverse momentum conservation. However, the power n deceases to 1.54 $\pm$ 0.18 when 10% initial charge separation is included. In addition, we found that the charge correlations depend very weakly on $p_- = |p_{t,\alpha} - p_{t,\beta}|$. In particular, the opposite-charge correlation increases gradually to a level of about 0.1×10^{-3} while the same-charge correlation stays at a constant level of about 0.25×10^{-3}. Even though the magnitude of the same-charge correlation is smaller than the experimental data, the integrated value is consistent

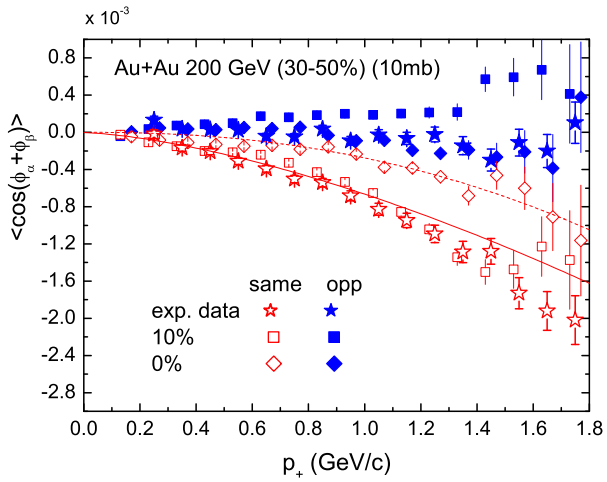

Figure 5: $\langle\cos(\phi_\alpha + \phi_\beta)\rangle$ as a function of $p_+ = (p_{t,\alpha}+p_{t,\beta})/2$ in AMPT calculations without (0%, diamonds) and with (10%, squares) initial charge separation for the 30-50% centrality bin in Au+Au collisions at $\sqrt{s_{\rm NN}}$=200 GeV (with a 10 mb parton cross section). The curves are power-law fits for the same-charge correlations from the AMPT calculations without (dash) and with (solid) initial charge separation, and the stars represent experimental data. Some points are slightly shifted for clarity.

with experimental data because the lowest p_- bin carries the highest weight.

Fig. 6 presents charge correlations as functions of the pseudorapidity difference ($\Delta\eta = |\eta_\alpha - \eta_\beta|$) of two final charged pions for the 30-50% centrality bin. Again we see that results from the AMPT model without initial charge separation can describe the opposite-charge correlation, while initial charge separation is needed to reproduce the same-charge correlation data. It is worth mentioning that the strong dependence on the pseudorapidity difference cannot be obtained in the present calculations from transverse momentum conservation [11]. More realistic longitudinal dynamics in the AMPT model contributes to the better description of the dependence on the pseudorapidity difference.

In addition to the angular correlation $\langle\cos(\phi_\alpha + \phi_\beta)\rangle$, charge separation also shows up in the angular correlation $\langle\cos(\phi_\alpha - \phi_\beta)\rangle$. The former is free of reaction plane independent backgrounds while the latter is also sensitive to reaction plane independent backgrounds. Charge separation increases the opposite-charge correlation and decreases the same-charge correlation for the

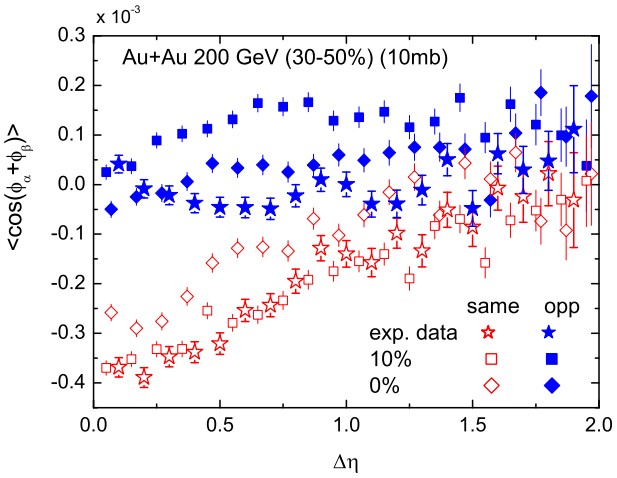

Figure 6: $\langle\cos(\phi_\alpha + \phi_\beta)\rangle$ as a function of $\Delta\eta = |\eta_\alpha - \eta_\beta|$ in AMPT calculations without (0%, diamonds) and with (10%, squares) initial charge separation for the 30-50% centrality bin in Au+Au collisions at $\sqrt{s_{\rm NN}}$=200 GeV (with a 10 mb parton cross section). The stars represent experimental data. Some points are slightly shifted for clarity.

former, while it decreases the opposite-charge correlation and increases the same-charge correlation for the latter. We will look at the centrality dependence of the charge correlation $\langle\cos(\phi_\alpha - \phi_\beta)\rangle$ in Fig. 7. When there is no initial charge separation, the AMPT results have the same trends as the experimental data for both the same-charge and the opposite-charge correlations. However, the correlations are much lower than those observed experimentally. Charge separation brings the same-charge correlation closer to data and the opposite-charge correlation farther away from data by amounts comparable to those for $\langle\cos(\phi_\alpha + \phi_\beta)\rangle$. However, the changes are not enough to make up for the large difference between the AMPT results and the experimental data. Additional backgrounds that can significantly increase the correlations are needed in order to describe the data.

4. Conclusions

In summary, final state interactions play an important role on charge separation in relativistic heavy-ion collisions. Parton cascade and resonance decay significantly reduce the charge separation from 10% in the initial state

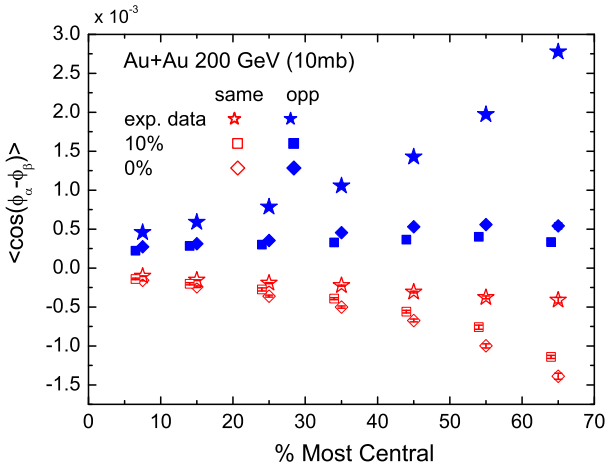

Figure 7: Centrality dependence of $\langle\cos(\phi_\alpha - \phi_\beta)\rangle$ from AMPT calculations without (0%, diamonds) and with (10%, squares) initial charge separation in Au+Au collisions at $\sqrt{s_{\rm NN}}$=200 GeV (with a 10 mb parton cross section). The stars represent experimental data. Some points are slightly shifted for clarity.

to 1-2% in the final state. Therefore, it is essential to take these final state effects into account for studies related to charge separation. Our results also suggest that mechanisms beyond transverse momentum conservation will be needed even for the description of the same-charge correlation.

Our approach includes the effects of local charge conservation and transverse momentum conservation automatically. However, detailed magnetic field evolution [37], or fluctuating domain sizes, or different topological charges are not included. These effects can lead to different charge separation percentages for different centralities. But they are not likely to help improve the simultaneous description of both the same-charge and opposite-charge correlations, and both $\langle\cos(\phi_\alpha + \phi_\beta)\rangle$ and $\langle\cos(\phi_\alpha - \phi_\beta)\rangle$. Schlichting and Pratt recently demonstrated that charge balancing can affect the difference between the opposite-charge and same-charge correlations [13]. This and other possible mechanisms certainly deserve further study for a satisfactory understanding of experimental data.

Acknowledgements

We thank A. Bzdak, C.M. Ko, V. Koch, J. Liao, Y.G. Ma, F. Wang for helpful discussions and the U.S. National Energy Research Scientific Computing Center for providing computing resources. This work was supported by the NSFC of China under Projects Nos. 10705044, 11035009, the Knowledge Innovation Project of Chinese Academy of Sciences under Grant No. KJCX2-EW-N01 (G.L.M.), and by the U.S. National Science Foundation under Grant Nos. PHYS-0554930 and PHYS-0970104 (B.Z.).

References

[1] B. I. Abelev *et al.* [STAR Collaboration], Phys. Rev. Lett. **103** (2009) 251601 [arXiv:0909.1739 [nucl-ex]].

[2] B. I. Abelev *et al.* [STAR Collaboration], Phys. Rev. C **81** (2010) 054908 [arXiv:0909.1717 [nucl-ex]].

[3] D. Kharzeev, R. D. Pisarski and M. H. G. Tytgat, Phys. Rev. Lett. **81** (1998) 512 [arXiv:hep-ph/9804221].

[4] D. Kharzeev, Phys. Lett. B **633** (2006) 260 [arXiv:hep-ph/0406125].

[5] D. E. Kharzeev, L. D. McLerran and H. J. Warringa, Nucl. Phys. A **803** (2008) 227 [arXiv:0711.0950 [hep-ph]].

[6] K. Fukushima, D. E. Kharzeev and H. J. Warringa, Phys. Rev. D **78** (2008) 074033 [arXiv:0808.3382 [hep-ph]].

[7] A. Bzdak, V. Koch and J. Liao, Phys. Rev. C **81** (2010) 031901 [arXiv:0912.5050 [nucl-th]].

[8] K. Fukushima, D. E. Kharzeev and H. J. Warringa, Phys. Rev. Lett. **104** (2010) 212001 [arXiv:1002.2495 [hep-ph]].

[9] G. Basar, G. V. Dunne and D. E. Kharzeev, Phys. Rev. Lett. **104** (2010) 232301 [arXiv:1003.3464 [hep-ph]].

[10] B. Müller and A. Schäfer, Phys. Rev. C **82** (2010) 057902 [arXiv:1009.1053 [hep-ph]].

[11] A. Bzdak, V. Koch and J. Liao, Phys. Rev. C **83** (2011) 014905 [arXiv:1008.4919 [nucl-th]].

[12] F. Wang, Phys. Rev. C **81** (2010) 064902 [arXiv:0911.1482 [nucl-ex]].

[13] S. Schlichting and S. Pratt, Phys. Rev. C **83** (2011) 014913 [arXiv:1009.4283 [nucl-th]].

[14] B. Zhang, C. M. Ko, B. A. Li and Z. W. Lin, Phys. Rev. C **61** (2000) 067901 [arXiv:nucl-th/9907017].

[15] Z. W. Lin, S. Pal, C. M. Ko, B. A. Li and B. Zhang, Nucl. Phys. A **698** (2002) 375 [arXiv:nucl-th/0105044].

[16] Z. W. Lin, C. M. Ko, B. A. Li, B. Zhang and S. Pal, Phys. Rev. C **72** (2005) 064901 [arXiv:nucl-th/0411110].

[17] X. N. Wang and M. Gyulassy, Phys. Rev. D **44** (1991) 3501.

[18] M. Gyulassy and X. N. Wang, Comput. Phys. Commun. **83** (1994) 307 [arXiv:nucl-th/9502021].

[19] B. Zhang, Comput. Phys. Commun. **109** (1998) 193 [arXiv:nucl-th/9709009].

[20] T. Sjöstrand, Comput. Phys. Commun. **82** (1994) 74.

[21] B. A. Li and C. M. Ko, Phys. Rev. C **52** (1995) 2037 [arXiv:nucl-th/9505016].

[22] Z. W. Lin and C. M. Ko, Phys. Rev. C **65** (2002) 034904 [arXiv:nucl-th/0108039].

[23] L. W. Chen and C. M. Ko, Phys. Rev. C **73** (2006) 044903 [arXiv:nucl-th/0602025].

[24] J. H. Chen *et al.*, Phys. Rev. C **74** (2006) 064902.

[25] B. Zhang, L. W. Chen and C. M. Ko, Phys. Rev. C **72** (2005) 024906 [arXiv:nucl-th/0502056].

[26] B. Zhang, C. M. Ko, B. A. Li, Z. W. Lin and B. H. Sa, Phys. Rev. C **62** (2000) 054905 [arXiv:nucl-th/0007003].

[27] B. Zhang, C. M. Ko, B. A. Li, Z. W. Lin and S. Pal, Phys. Rev. C **65** (2002) 054909 [arXiv:nucl-th/0201038].

[28] B. Zhang, Phys. Lett. B **647** (2007) 249 [arXiv:nucl-th/0606039].

[29] Z. W. Lin, C. M. Ko and S. Pal, Phys. Rev. Lett. **89** (2002) 152301 [arXiv:nucl-th/0204054].

[30] S. Zhang *et al.*, Phys. Rev. C **76** (2007) 014904 [arXiv:0706.3820 [nucl-th]].

[31] S. Pal, Phys. Rev. C **80** (2009) 041901.

[32] J. Xu and C. M. Ko, Phys. Rev. C **83** (2011) 021903. [arXiv:1011.3750 [nucl-th]].

[33] G. L. Ma and X. N. Wang, arXiv:1011.5249 [nucl-th].

[34] S. A. Voloshin, Phys. Rev. C **70** (2004) 057901 [arXiv:hep-ph/0406311].

[35] S. Pratt, arXiv:1002.1758 [nucl-th].

[36] S. Pratt, S. Schlichting and S. Gavin, arXiv:1011.6053 [nucl-th].

[37] V. D. Toneev and V. Voronyuk, arXiv:1012.1508 [nucl-th].